

Charge-Orbital Ordering and Verwey Transition in Magnetite

Hong-Tay Jeng,^{1,*} G. Y. Guo,^{2,3,†} and D. J. Huang³

¹*Physics Division, National Center for Theoretical Sciences, Hsinchu 300, Taiwan*

²*Department of Physics, National Taiwan University, Taipei 106, Taiwan*

³*National Synchrotron Radiation Research Center, Hsinchu 30077, Taiwan*

(Received 4 February 2004; published 5 October 2004)

Local density approximation + Hubbard U (LDA + U) band structure calculations reveal that magnetite (Fe_3O_4) forms an insulating charge-orbital-ordered state below the Verwey transition temperature. The calculated charge ordering is in good agreement with that inferred from recent experiments. We found an associated t_{2g} orbital ordering on the octahedral Fe^{2+} sublattice. Such an orbital ordering results primarily from the on-site Coulomb interaction. This finding unravels such fundamental issues about the Verwey transition as the mechanism for the charge ordering and for the formation of the insulating gap, as well as the nonobedience of the Anderson's criterion for the charge ordering.

DOI: 10.1103/PhysRevLett.93.156403

PACS numbers: 71.20.-b, 31.15.Ar, 32.10.Dk

Some transition-metal oxides exhibit spatial localization of the charge carriers on certain ionic sites (charge ordering), as observed in many magnetoresistive manganites [1] and superconducting cuprates [2]. Charge ordering is typically accompanied by real space ordering of the charge carriers in certain orbitals (orbital ordering). The electric transport and magnetic properties of transition-metal oxides are intimately related to charge and orbital ordering [3]. For example, dynamic fluctuations of charge ordered stripes have been proposed as a mechanism of high temperature (T) superconductivity [4]. Therefore, there have been intensive efforts—both experimental and theoretical—to unravel the mechanisms giving rise to such intriguing phenomena. The classic charge ordering problem is that of magnetite, which, however, has been unresolved for over 60 years.

Magnetite has been considered as a mixed-valence $3d$ transition-metal compound with the formal chemical formula $\text{Fe}_A^{3+}[\text{Fe}^{2+}\text{Fe}^{3+}]_B\text{O}_4$ [5]. At room- T , magnetite crystallizes in the cubic inverted spinel structure with tetrahedral A sites occupied by one-third of the Fe ions as Fe^{3+} , and octahedral B sites occupied by the remaining Fe ions with equal numbers of Fe^{2+} and Fe^{3+} . Below 860 K, magnetite is a ferrimagnet with the B cation magnetic moments aligned antiparallel to the A cation moments. It is a metal with a moderate electronic conductivity.

Verwey found that magnetite undergoes a first-order phase transition on cooling below ~ 120 K (T_V), at which the electrical conductivity abruptly decreases by 2 orders of magnitude [6], and the structure changes from the cubic symmetry [5]. Assuming the high- T conductivity is due to fast electron hopping between the B Fe^{2+} and Fe^{3+} ions, Verwey *et al.* [5] interpreted this metal-insulator transition (Verwey transition) as a charge ordering of the Fe^{2+} and Fe^{3+} states on the B sites in successive (001) planes, resulting in an orthorhombic structure (Verwey model). However, the Verwey model was later disproved by experiments [7]. Surprisingly, despite inten-

sive investigations in the past 60 years [7], fundamental questions about the Verwey transition such as the existence [8,9] and origin [7] of the charge ordering, the thermodynamic nature [10], the nature of the electronic state, and the mechanism for the formation of the insulating gap [7] below T_V , remain unresolved.

Recently Wright *et al.* [11] have refined the low- T structure of magnetite using high-resolution neutron and x-ray powder-diffraction data and found evidence for charge ordering which, however, is much more complicated than the Verwey model [5] and does not meet Anderson's condition of minimal electrostatic repulsion [12]. In this Letter, we present electronic structure calculations within local density approximation (LDA) with generalized gradient correction (GGA) [13] plus on-site Coulomb interaction U (LDA + U) [14–16] using this refined crystal structure [11]. We find not only a charge ordering which is consistent with the experiments but also an associated orbital ordering. The finding of this charge-orbital ordering enables us to gain insight into several long-standing issues about the Verwey transition.

The low- T crystal structure of magnetite [11] used in our calculations is a complex monoclinic $P2_1/c$ structure with 56 atoms per unit cell, as shown in Fig. 1(a). The B Fe sites split into six inequivalent sites, namely, $B1a$, $B1b$, $B2a$, $B2b$, $B3$, and $B4$ [see Fig. 1(a) and [11]]. We performed LDA + U calculations by using the highly accurate full-potential projected augmented wave method [17] as implemented in the VASP package [18]. A cutoff energy of 400 eV for plane waves is used. A $6 \times 6 \times 2$ Monkhorst-Pack k -point grid in the Brillouin zone was used. Coulomb energy $U = 4.5$ eV [19] and exchange parameter $J = 0.89$ eV [14] were used for all Fe ions.

The calculated LDA + U density of states of Fe_3O_4 in both the cubic and monoclinic structures are shown in Fig. 2. Similar to previous LDA calculations [20], the LDA + U band structure calculations show that the cubic Fe_3O_4 is a metal with the Fermi level sitting in the middle of the spin-down B Fe t_{2g} band [Fig. 2(a) and [20]]. The

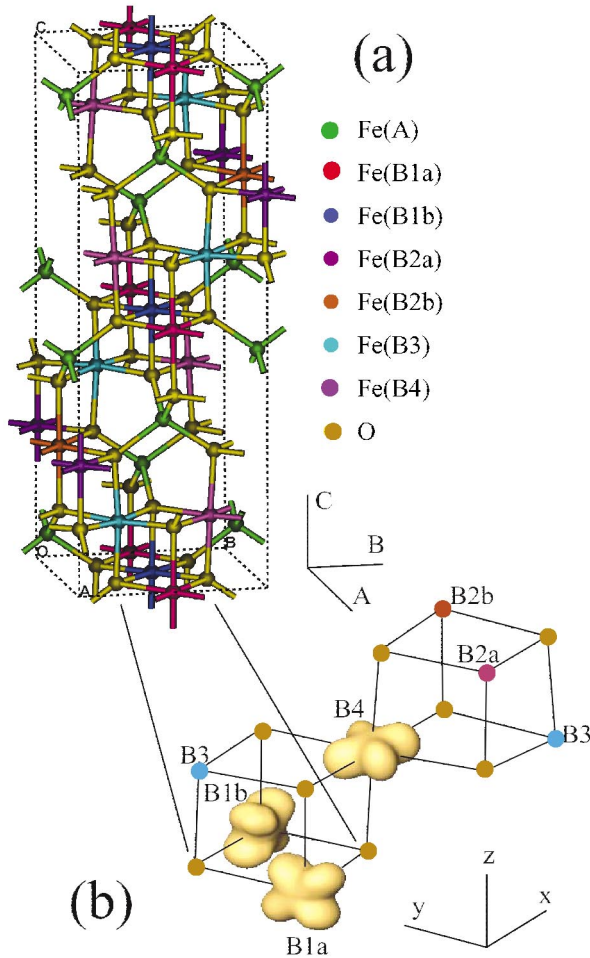


FIG. 1 (color). (a) Crystal structure of the monoclinic Fe_3O_4 . (b) Orbital ordering in B -site sublattice. x - y - z and a - b - c are, respectively, the local and global coordinates.

spin-up B Fe $3d$ band and the spin-down A Fe $3d$ band are completely filled, being at least 1.5 eV below the Fermi level, in accordance with Hund's rule. Figure 2 shows that an energy gap is opened at the Fermi level as the cubic structure is transformed into the monoclinic structure. This insulating gap is small (0.2 eV) but consistent with the experimental gap of ~ 0.1 eV from, e.g., photoemission and optical measurements [21].

Evidence for the charge ordering in the low- T structure of magnetite comes from the calculated valence charges on the B Fe ions within the atomic spheres of radius 1.0 Å. Table I shows that the B Fe ions can be divided into two groups according to their valence charges, namely, the electron-rich $B1$ and $B4$ Fe ions with a lower ionicity of +2.4 and the electron-poor $B2$ and $B3$ Fe ions with a higher ionicity of +2.6. This charge order is consistent with the observed bond-length order of the B Fe ions [11] that the B Fe ions with lower and higher ionicities result in expanded (~ 2.07 Å) and contracted (~ 2.05 Å) BO_6 octahedra due to the weaker and stronger Coulomb attractions between the B cations and neighbor-

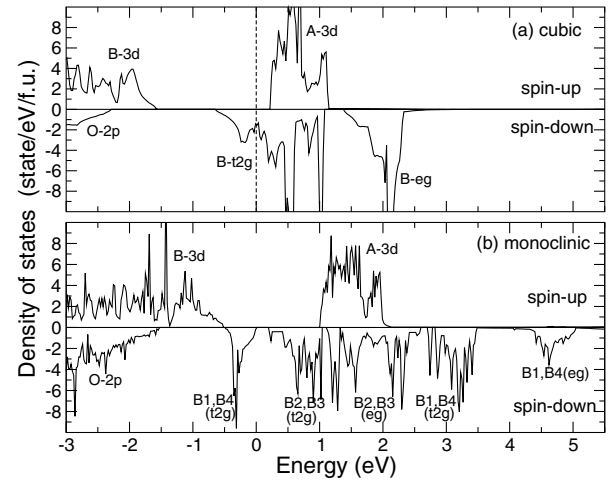


FIG. 2. Spin-resolved density of state of Fe_3O_4 in (a) the high- T cubic structure and (b) the low- T monoclinic structure. The Fermi level is at zero energy.

ing O^{2-} anions, respectively. Interestingly, this charge ordering is accompanied by a spin ordering. Table I indicates that the $B2$ and $B3$ Fe ions are in a higher spin state, whereas the $B1$ and $B4$ Fe ions have a smaller spin moment due to the extra spin-down electrons. Furthermore, the charge (spin) ordering can be considered as the superposition of $[001]_c$ and $[00\frac{1}{2}]_c$ charge (spin) density wave modulations, as pointed by Wright *et al.* [11]. Note that the charge separation between the two B Fe ion groups is far less than the nominal ionicity difference of $+1e$ between the Fe^{3+} and Fe^{2+} . Nonetheless, this is consistent with the small charge separation between the so-called Mn^{3+} and Mn^{4+} in manganites found in previous electronic structure calculations [22,23]. Furthermore, both the pattern and charge separation of the calculated charge ordering agrees well with that inferred from the neutron and x-ray diffraction experiments [11] (Table I). In the rest of this Letter, we label $B1$ and $B4$ Fe ions as Fe^{2+} and $B2$ and $B3$ Fe ions as Fe^{3+} for simplicity.

To identify the origin of the charge ordering, we project the density of states around the Fermi level (Fig. 2) onto the five $3d$ orbitals of the six inequivalent B Fe ions, as shown in Fig. 3(a). The local coordinates are used with the z axis pointing to the crystal c axis and the x and y axes directed to the neighboring O ions in the crystal a - b plane (Fig. 1). It is clear from Fig. 3(a) that the B Fe^{2+}

TABLE I. Charge (e) and moment (μ_B) of the B Fe ions within the atomic spheres of radius 1.0 Å in monoclinic Fe_3O_4 .

	Expt. (Ref. [11]) valence charge	LDA + U valence charge	LDA + U spin moment
Fe($B1$)	5.6	5.57	3.45
Fe($B2$)	5.4	5.41	3.90
Fe($B3$)	5.4	5.44	3.81
Fe($B4$)	5.6	5.58	3.39

ions have a narrow spin-down $3d-t_{2g}$ band right below the Fermi level with a bandwidth of ~ 0.5 eV, whereas such a sharp band is absent in the B Fe^{3+} ions. Remarkably, these extra bands of the $B1a$, $B1b$, and $B4$ Fe^{2+} ions are, respectively, of predominant d_{yz} , d_{xz} , and d_{xy} characters, with an integrated charge of $0.59e$, $0.59e$, and $0.63e$, respectively [Fig. 3(a)]. This indicates the formation of the spin-down t_{2g} orbital-ordered state in which the B Fe^{2+} ions each has one spin-down t_{2g} orbital occupied, whereas all the spin-down t_{2g} orbitals of the B Fe^{3+} ions are empty, as illustrated in Fig. 3(b). In this context, labeling the electron-rich $B1$ and $B4$ Fe ions as Fe^{2+} and the electron-poor $B2$ and $B3$ Fe ions as Fe^{3+} mentioned above makes sense. Nevertheless, this t_{2g} orbital ordering is strongly screened and thus the resultant charge differences between B Fe^{3+} and Fe^{2+} ions are far short of one electron (Table I). To see clearly the orbital ordering, in Fig. 1(b) we have plotted the charge-density contours corresponding to the narrow B Fe t_{2g} band just below the Fermi level [Fig. 2(b)]. Indeed, we find a crosslike charge-density distribution on each B Fe^{2+} ion [as shown in Fig. 1(b)] which is absent on all the other types of the

ions (B Fe^{3+} as well as O and A Fe^{3+} ions). In short, there is an orbital ordering of conduction electrons in the B Fe^{2+} t_{2g} orbitals in magnetite below T_V which drives the charge ordering.

In the cubic structure of magnetite, the oxygen and B Fe atoms form a network of corner-sharing B_4O_4 cubes consisting of interpenetrating B_4 and O_4 tetrahedra (Fig. 1). Below T_V , the charge ordering gives rise to two different groups of the B_4O_4 cubes, namely, electron-rich cubes each having three $B(Fe^{2+})$ and one $B(Fe^{3+})$ ions, and electron-poor cubes each containing three $B(Fe^{3+})$ and one $B(Fe^{2+})$ ions [11]. A pronounced structural distortion observed in the low- T phase magnetite is the large inwards displacement of $B3$ Fe^{3+} along the cube diagonal [11]. Let us focus on an electron-rich cube, e.g., the lower cube in Fig. 1(b). In this cube, each of the three B Fe^{2+} sites has one of the three t_{2g} orbitals occupied such that one lobe of the t_{2g} orbital pointing towards the B Fe^{3+} site [Fig. 1(b)]. Clearly, when the $B3$ Fe^{3+} ion is pulled inwards along the cube diagonal, the energy will be lowered due to the increased intersite Coulomb attraction between the $B3$ Fe^{3+} and the t_{2g} orbital electron clouds of $Fe^{2+}(B1a)$, $Fe^{2+}(B1b)$, and $Fe^{2+}(B4)$ ions. This explains the most significant atomic position deformation observed upon cooling through the Verwey transition [11]. Indeed, our LDA + U calculations shows that the total energy of Fe_3O_4 in the monoclinic structure is 0.35 eV/f.u. (formula unit) lower than in the cubic structure. On the other hand, this atomic displacement of the $B3$ Fe^{3+} strengthens the orbital ordering by lowering the energy of the occupied B Fe^{2+} t_{2g} orbitals and raising the energy of the unoccupied t_{2g} as well as e_g orbitals of B Fe^{2+} ions, as illustrated in Fig. 3(b).

Another interesting issue is why the charge ordering pattern observed recently [11] does not satisfy Anderson's criterion [12] which requires that each corner-sharing B Fe tetrahedron should contain two Fe^{2+} and two Fe^{3+} ions in order to minimize the electrostatic energy. Anderson's criterion has been used to screen many charge ordering models proposed for magnetite [8]. Our finding of the charge-orbital ordering offers an explanation. In Anderson's calculations [12], the charges in ferrites are treated as the point charges and thus the electrostatic energy depends only on the number of divalent-trivalent cation-pairs. As a result, putting two Fe^{2+} and two Fe^{3+} on each B Fe tetrahedron would maximize the number of Fe^{2+} - Fe^{3+} pairs and give rise to the lowest energy. However, this point charge assumption of Anderson is certainly inappropriate for the low- T magnetite which is in the charge-orbital-ordered state. In particular, the obtained orbital ordering would give rise to additional intersite Coulomb attraction between the B Fe^{3+} ions and B Fe^{2+} ions and stabilize the observed charge ordering pattern, as discussed above.

Both the GGA calculations (i.e., $U = J = 0.0$) with the distorted lattice and the LDA + U calculations without

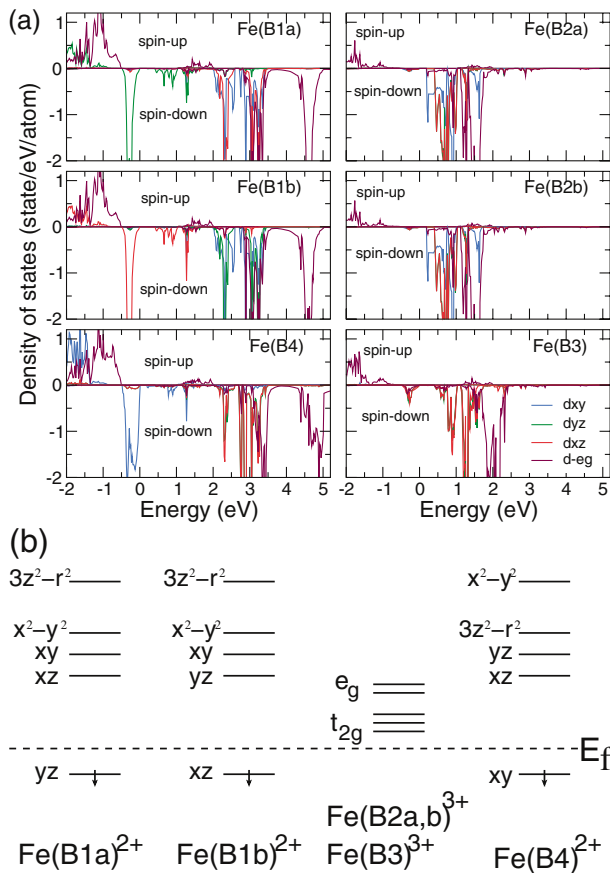


FIG. 3 (color). (a) Density of states of Fe_3O_4 in the monoclinic structure projected onto the B Fe d orbitals. The Fermi level E_f is at the zero energy. (b) Schematic energy level diagram for the spin-down B Fe d orbitals in the monoclinic Fe_3O_4 .

the structural distortion (i.e., using the $a_c/\sqrt{2} \times a_c/\sqrt{2} \times 2a_c$ supercell of the cubic structure with lattice constant a_c) give rise to a metallic band structure. Importantly, the charge-orbital ordering still occurs in the latter with smaller charge separations of $\sim 0.1e$ and much reduced density of states at the Fermi level, whereas it is absent in the former (the charge separations being less than $0.03e$). Thus, the on-site Coulomb correlations of the Fe-3d electrons play an important role in the charge-orbital ordering and hence the Verwey transition [24]. Nevertheless, the insulating gap occurs when the structural distortion is also taken into account.

We notice that the electronic structure of magnetite has been studied within the LDA + U scheme before by Anisimov *et al.* [19] and Antonov *et al.* [25]. However, to obtain the insulating charge ordered state of the Verwey type, Anisimov *et al.* [19] introduced not only the on-site Coulomb interaction U as in the LDA + U scheme but also the so-called intersite Coulomb interaction which, in principle, is already included in self-consistent band structure calculations. Antonov *et al.* [25], on the other hand, explicitly applied two kinds of U to the prescribed B Fe²⁺ and Fe³⁺ ions. In both cases, as expected, a small gap of 0.34 eV [19] and 0.19 eV [25] is obtained. Nonetheless, the simple Verwey charge ordering model used is incompatible with experiments [7,11]. In contrast, in the present “first-principles” LDA + U calculations, a single on-site Coulomb interaction U is used for all the Fe ions in magnetite, and an insulating charge ordered state which is consistent with the recent experiments comes out naturally. Furthermore, an orbital ordering is found, as described in the preceding paragraphs.

To summarize, we have investigated the electronic structure of magnetite using the recently refined low- T structure within the LDA + U formalism. We found an insulating charge ordered ground state whose configuration and charge separation are in good agreement with that inferred from recent powder-diffraction measurements. More importantly, we also found that below T_V , conduction electrons form a t_{2g} orbital-ordered state by occupying spin-down d_{yz} , d_{xz} , and d_{xy} orbitals on different B Fe²⁺ sublattices. This finding of the orbital-ordered state in the low- T structure magnetite resolves several fundamental issues about the Verwey transition such as the nature of the low- T electronic state, the driving force of the charge ordering, and also the question that why Anderson’s criterion for the charge ordering breaks down.

We thank K. Terakura, I.V. Solovyev, F.C. Zhang, and A. Fujimori for valuable discussions. This work was supported by the National Science Council of Taiwan.

*Electronic address: jeng@phys.nthu.edu.tw

†Electronic address: gyguo@phys.ntu.edu.tw

- [1] S. Mori, C. H. Chen, and S.W. Cheong, *Nature* (London) **392**, 473 (1998).
- [2] J. M. Tranquada *et al.*, *Nature* (London) **375**, 561 (1995).
- [3] Y. Tokura and N. Nagaosa, *Science* **288**, 462 (2000).
- [4] M. I. Salkola, V. J. Emery, and S. A. Kivelson, *Phys. Rev. Lett.* **77**, 155 (1996).
- [5] E. J. W. Verwey and P. W. Haayman, and F. C. Romeijn, *J. Chem. Phys.* **15**, 181 (1947).
- [6] E. J. W. Verwey, *Nature* (London) **375**, 561 (1995).
- [7] See the review of research on the Verwey transition: J. García and G. Subías, *J. Phys. Condens. Matter* **16**, R145 (2004); F. Walz, *J. Phys. Condens. Matter* **14**, R285 (2002).
- [8] J. M. Zuo, J. C. H. Spence, and W. Petuskey, *Phys. Rev. B* **42**, 8451 (1990).
- [9] J. García *et al.*, *Phys. Rev. Lett.* **85**, 578 (2000).
- [10] J. P. Shepherd *et al.*, *Phys. Rev. B* **43**, 8461 (1991).
- [11] J. P. Wright, J. P. Attfield, and P. G. Radaelli, *Phys. Rev. Lett.* **87**, 266401 (2001); *Phys. Rev. B* **66**, 214422 (2002).
- [12] P. W. Anderson, *Phys. Rev.* **102**, 1008 (1956).
- [13] J. P. Perdew and Y. Wang, *Phys. Rev. B* **45**, 13 244 (1992).
- [14] V. I. Anisimov, J. Zaanen, and O. K. Andersen, *Phys. Rev. B* **44**, 943 (1991).
- [15] A. I. Liechtenstein, V. I. Anisimov, and J. Zaanen, *Phys. Rev. B* **52**, R5467 (1995).
- [16] In principle, our calculations should be denoted as GGA + U . Nonetheless, following the tradition, we use LDA + U here.
- [17] P. E. Blöchl, *Phys. Rev. B* **50**, 17 953 (1994); G. Kresse and J. Joubert, *Phys. Rev. B* **59**, 1758 (1999).
- [18] G. Kresse and J. Hafner, *Phys. Rev. B* **48**, 13 115 (1993); G. Kresse and J. Furthmüller, *Comput. Mater. Sci.* **6**, 15 (1996); *Phys. Rev. B* **54**, 11169 (1996).
- [19] V. I. Anisimov *et al.*, *Phys. Rev. B* **54**, 4387 (1996).
- [20] See, e.g., H.-T. Jeng and G. Y. Guo, *Phys. Rev. B* **65**, 94429 (2002), and references therein.
- [21] S. K. Park, T. Ishikawa, and Y. Tokura, *Phys. Rev. B* **58**, 3717 (1998).
- [22] P. Mahadevan, K. Terakura, and D. D. Sarma, *Phys. Rev. Lett.* **87**, 66404 (2001).
- [23] D. J. Huang *et al.*, *Phys. Rev. Lett.* **92**, 87202 (2004).
- [24] LDA + U calculations for the low- T structure have also been performed using (i) $U = 5.0$ eV, $J = 0.89$ eV, and GGA exchange-correlation (x-c) potential, (ii) $U = 4.5$ eV, $J = 0.5, 0.7, 1.1$ eV and GGA x-c potential, and (iii) $U = 4.5, 5.0, 5.5$ eV, $J = 0.89$ eV and LDA x-c potential. In all the cases, the charge-orbital ordering is obtained with the charge separations being within $0.1 \sim 0.2e$, indicating that it is robust with respect to GGA or LDA x-c potential and also to the reasonable variation of U and J used.
- [25] V. N. Antonov *et al.*, *Phys. Rev. B* **64**, 134410 (2001).